International Journal of Multiphysics
Volume 18, No. 3, 2024
ISSN: 1750-9548

Numerical Calculation Method of Multi-Scale Seepage Equation Considering Langmuir Desorption of Shale Gas

Zuocai Liao[1], Hongtao Zhou[2,*]

[1] Karamay Vocational & Technical College, Karamay 834000, China.

[2] China University of Petroleum-Beijing at Karamay 834000, China.

*Corresponding Author.

Abstract

Utilizing Besok-Karniadakist's motion equations for ultra-low permeability shale gas reservoirs, which accommodate four flow modes, and incorporating the Langmuir adsorption, transportdiffrential equations are derived. A pseudo-pressure formulation adhering to Darcy's law and a pseudo-time are introduced. By applying the mass conservation, a correspondence between nonlinear and linear equation parameters is established, merging both types of equations. Through examples, the production dynamics of nonlinear seepage, including fixed well-bottom pressure and production rates, and parameter sensitivity are analyzed, offering insights for enhancing shale gas productivity.

Keywords: Shale gas reservoir, langmuir adsorption, quasi-time transform function, mass conservation equation of quasi-time transformation.

1. Introduction

Shale gas percolation in China has been studied extensively. However, these seepage models are based on the seepage equation of tight gas [1-3], which is different from the micro-scale of shale gas reservoir, so Knudsen diffusion is considered and Langmuir instantaneous desorption is treated as the source and sink term, while the surface diffusion and gas slip of adsorbed gas, as well as the dynamic equilibrium process between adsorption and desorption are ignored, so there are shortcomings. Shale gas belongs to a special branch of gas percolation. Its composition is more monolithic than that of ordinary gas. Its reservoir formation mechanism and flow mechanism have been intensively studied by scholars from home and abroad. Although the analytical approach is described by the previous equation, it is still of positive interest to predict the time-dependent production and pressure variations and the influence factors by considering adsorption-desorption and constructing a model of unsteady percolation that fully takes desorption, diffusion and slip into account.

Michel [4] and others [5-9] use the improved shale gas transport equation to describe the gas flow in nano-scale non-Darcy permeability media, and its flow in the matrix includes viscous flow of free gas, Knudsen diffusion and surface diffusion and slip of adsorbed gas. The mechanism represented by equation is more comprehensive and well-established, which makes it possible to solve it analytically. Starting from the ideal gas flow of a single capillary, this paper extends to the whole capillary tube bundle model, determines the absolute permeability and apparent permeability of the formation by combining the theory of probability and statistics, and redefines the molecular mean free path to describe the behavior characteristics of real gas in the reservoir. The model and computational ideas presented in this paper are very instructive for shale gas development. After studying the paper, it was found that the authors had simplified the permeability correction coefficients in order to introduce a new pseudo-pressure function and solve the equations. Here we present a solution method that is faithful to the original parametric relations of the percolation equation and is based on quasi-time transformation functions.

2. Review of Basic Theory

Beskok and Karniadakis (1999) put forward a formula for gas flow in porous media with extremely low permeability, and Michel improved the formula. The modified model is suitable for four flow patterns, which are as follows.

$$v = -\frac{1}{8}\frac{r^2}{\mu}\left(1+\alpha K_n\right)\left(1+\frac{4K_n}{1-bK_n}\right)\frac{dP}{dx} \tag{1}$$

Knudsen number K_n is determined by the following formula:

$$K_n = \frac{\lambda}{r} \tag{2}$$

Where λ is the average free path of molecules, m ; r is defined as the comprehensive pore throat radius including cracks and pores, m ;.

The absolute permeability is determined by the following formula:

$$k_0 = \frac{r^2}{8} \tag{3}$$

Obviously, formula (1) can be regarded as Darcy's formula with two amendments. The slip coefficient b is -1. The thinning coefficient α is determined by the following relation:

$$\alpha = \frac{128}{15\pi^2}\tan^{-1}(4K_n^{0.4}) \tag{4}$$

The free path of the real gas has been expanded to accommodate the calculation of the normal pressure condition, which is given by the following equation:

$$\lambda = \sqrt{\frac{\pi RT}{2M_w}}\frac{\mu z}{P} \tag{5}$$

The mean velocity of the true gas was derived by the original authors and given in the following form:

$$\bar{u} = \sqrt{\frac{8zRT}{\pi M_w}} \tag{6}$$

The molecular density ρ is given by the following formula:

$$\rho = \frac{M_w P}{zRT} \tag{7}$$

Combining the mean free path expression given by Guggenheim (1960) and Knudsen diffusion coefficient D_k given by Civan (2010b), the formula (1) can be rewritten as:

$$v = -\frac{K_0}{\mu}\left(1+\frac{3\pi}{2}\frac{\mu}{r^2}D_k\frac{1}{p}\right)\frac{dp}{dx} \tag{8}$$

Both sides of Equation (8) can be multiplied by the density to obtain the mass flow in the following form:

$$\Gamma = \rho v = -\rho \frac{K_0}{\mu} \frac{dp}{dx} - \frac{3\pi}{18} D_k \frac{d\rho}{dx} \tag{9}$$

The mass flow includes a convective term following Darcy's law plus a diffusion term following Fick's law. It can accommodate the entire range of flow patterns. Further analysis and description of the flow patterns can be found in the original article.3. Application and analysis of shale gas production

The permeability of shale gas reservoirs themselves is extremely low. Even allowing for the presence of micro-fractures, the pressure transport radius of gas wells is still very limited, and the output of ordinary vertical wells is not economically valuable. Real production wells typically employ hydraulic fracturing to shorten the pressure conduction path and provide underground high-speed flow channels for the produced shale gas. Multi-stage hydraulic fracturing is now widely used for shale gas. As a theoretical discussion, the vertical well model of a single hydraulic fracture well is still used in this paper to illustrate the application of the method. The complex fracture system can be computed using the Green's function method and numerically according to the linearized equations in this paper.

2.1 Establishment of Langmuir unsteady seepage model considering desorption

During the production process, the formation stress conditions, pore opening and formation pressure of the shale reservoir change over time, and the original equilibrium state will no longer exist; Shale gas is partially stored in the pore fracture medium and partially adsorbed in the matrix, which is analyzed because the adsorption capacity decreases due to pressure drop conduction, and gas in the pore fracture medium can also percolate. Although the adsorption capacity of shale gas decreases with the increase of temperature, storage can still be regarded as a constant temperature medium in general [10].

Langmuir gave the isothermal adsorption equation of pure gas:

$$V_E = V_L \left(\frac{\overline{p}}{\overline{p} + p_L} \right) \tag{10}$$

Where p_L is Langmuir pressure; V_L Is Langmuir volume, adsorption capacity per unit bedrock, m^3 / m^3; V_E Is the total adsorption volume, m^3 / m^3 ; For the average pressure, the adsorption-desorption process is regarded as a transient process, and the desorption amount varying with pressure can be expressed as:

$$V_d = V_L \left(\frac{p_{ini}}{p_{ini} + p_L} - \frac{\overline{p}}{\overline{p} + p_L} \right) \tag{11}$$

Where V_d is the cumulative desorption amount of matrix per unit volume; p_{ini} is the original gas reservoir pressure; $\overline{p}$ is the current average pressure of gas reservoir.

The research shows that $\overline{p}$ is generally replaced by the current formation pressure p , unless it enters the quasi-steady flow stage. Therefore, the above formula can be written as:

$$V_d = V_L \left(\frac{p_i}{p_i + p_L} - \frac{p}{p + p_L} \right) \tag{12}$$

In the presence of non-stationary percolation of shale gas, the diffuse flux per unit volume of bedrock can be described by the following formula according to Fick's law:

$$q_d = \rho_{gsc} \frac{\partial V_d}{\partial t} = \rho_{gsc} \left(\frac{\partial V_d}{\partial p} \right) \left(\frac{\partial p}{\partial t} \right) \tag{13}$$

Where ρ_{gsc} is the density of shale gas under ground standard conditions.

According to equations (8) and (3), the equation of motion can be expressed as:

$$v = -\frac{K_0}{\mu}\left(1+\frac{3\pi\alpha\mu D_k}{16K_0 p}\right)\left(\frac{dp}{dx}\right) \tag{14}$$

The continuity equation needs to add source and sink terms q_d :

$$-\frac{\partial\left(\rho_g v_x\right)}{\partial x}+q_d=\frac{\partial\left(\phi\rho_g\right)}{\partial t} \tag{15}$$

The density state of shale gas can be described by the following formula:

$$\rho_g=\frac{T_{sc}Z_{sc}\rho_{gsc}}{p_{sc}}\cdot\frac{p}{TZ} \tag{16}$$

In the production process, shale gas reservoir can be regarded as an isothermal medium, so its isothermal compressibility can be expressed as:

$$c(p)=\frac{-dV}{Vdp}|_{T=C}=\frac{1}{p}-\frac{1}{Z}\frac{dZ}{dp}|_{T=\mathrm{C}} \tag{17}$$

Substituting the equations of motion and state into the continuity equation;

$$\frac{\partial}{\partial x}\left(\frac{1}{\mu Z}\left(p+\frac{3\pi\alpha\mu D_k}{16K_0}\right)\left(\frac{\partial p}{\partial x}\right)\right)+\frac{p_{sc}T}{K_0T_{sc}Z_{sc}\rho_{gsc}}=\frac{\phi}{K_0}\frac{\partial}{\partial t}\left(\frac{p}{Z}\right) \tag{18}$$

Usually, the above formula is converted into cylindrical coordinates, and the underground flow of shale gas is described by plane radial flow:

$$\frac{1}{r}\frac{\partial}{\partial r}\left(r.\frac{1}{\mu Z}\left(p+\frac{3\pi\alpha\mu D_k}{16K_0}\right)\left(\frac{\partial p}{\partial r}\right)\right)+\frac{p_{sc}T}{K_0T_{sc}Z_{sc}\rho_{gsc}}=\frac{\phi}{K_0}\frac{\partial}{\partial t}\left(\frac{p}{Z}\right) \tag{19}$$

Combined with formula (17), the above formula can be transformed into:

$$\frac{1}{r}\frac{\partial}{\partial r}\left(r.\frac{1}{\mu Z}\left(p+\frac{3\pi\alpha\mu D_k}{16K_0}\right)\left(\frac{\partial p}{\partial r}\right)\right)+\frac{p_{sc}T}{K_0T_{sc}Z_{sc}\rho_{gsc}}q_d=\frac{\phi\mu c}{K_0}\frac{\partial}{\partial t}\left[\frac{p}{\mu Z}\frac{\partial p}{\partial t}\right] \tag{20}$$

It can be easily obtained from formula (12):

$$\frac{\partial V_d}{\partial p}=-\frac{p_L V_L}{\left(p+p_L\right)^2} \tag{21}$$

In this paper, when formula (21) is used for digital calculation, the original formation pressure is used. The errors are very small compared to the results of the mean pressure calculation for the ring formation. Therefore, it is appropriate to replace the average pressure obtained by complex calculations with the original formation pressure. Ignoring the two steps, rewrite equation (20) as follows:

$$\frac{1}{r}\frac{\partial}{\partial r}\left(r.\frac{1}{\mu Z}\left(p+\frac{3\pi\alpha\mu D_k}{16K_0}\right)\left(\frac{\partial\left(p+\frac{3\pi\alpha\mu D_k}{16K_0}\right)}{\partial r}\right)\right)+\frac{p_{sc}T}{K_0T_{sc}Z_{sc}\rho_{gsc}}\left(\frac{\partial V_d}{\partial p}\right)\frac{\partial}{\partial t}\left(p+\frac{3\pi\alpha\mu D_k}{16K_0}\right)$$
$$=\frac{\phi\mu c}{K_0}\left[\frac{p}{\mu Z}\frac{\partial\left(p+\frac{3\pi\alpha\mu D_k}{16K_0}\right)}{\partial t}\right] \tag{22}$$

2.2 Linearization method and digital solution of differential equation

Let $m=p+\frac{3\pi\alpha\mu D_k}{16K_0}$ be the composite pressure, then the formula (22) combined with the formula (21) can be written as [10]:

$$\frac{1}{r}\frac{\partial}{\partial r}\left(r.\frac{m}{\mu Z}\left(\frac{\partial m}{\partial r}\right)\right)-\frac{p_{sc}T}{K_0T_{sc}Z_{sc}\rho_{gsc}}\frac{p_LV_L}{\left(p+p_L\right)^2}\frac{\partial m}{\partial t}=\frac{\phi\mu c}{K_0}\left(\frac{p}{\mu Z}\frac{\partial m}{\partial t}\right) \tag{23}$$

The pseudo pressure function is introduced and defined as follows [10]:

$$\psi=2\int_{m_a}^{m}\frac{m}{\mu Z}dm=2\int_{p_a}^{p}\left(1+\frac{3\pi\phi}{16K_0}.\frac{\mu D_k}{p}\right)\frac{p}{\mu Z}dp \tag{24}$$

Where m_a is the composite pressure p_a under a specified pressure., Pa.

So according to equation (23), the differential equation expressed by pseudo pressure is:

$$\frac{1}{r}\frac{\partial}{\partial r}\left(r.\left(\frac{\partial\psi}{\partial r}\right)\right)-\frac{p_{sc}T}{K_0T_{sc}Z_{sc}\rho_{gsc}}\frac{p_LV_L}{\left(p+p_L\right)^2}\frac{1}{m}\frac{\partial\psi}{\partial t}=\frac{\phi\mu c}{K_0}\frac{p}{m}\left(\frac{\partial\psi}{\partial t}\right) \tag{25}$$

After finishing the above formula, you can get:

$$\frac{1}{r}\frac{\partial}{\partial r}\left(r.\left(\frac{\partial\psi}{\partial r}\right)\right)=\frac{\phi\mu}{K_0}\left(c_g+c_d\right)\left(\frac{\partial\psi}{\partial t}\right) \tag{26}$$

Among them:

$$c_g=c.\frac{p}{p+\frac{3\pi\alpha\mu D_k}{16K_0}} \tag{27}$$

$$c_d=\frac{p_{sc}TZ}{T_{sc}Z_{sc}\phi}\frac{p_LV_L}{\left(p+p_L\right)^2}\frac{1}{p+\frac{3\pi\alpha\mu D_k}{16K_0}} \tag{28}$$

Remember that $c_a=c_g+c_d$ will deform the right side of equation (26):

$$\frac{\phi\mu}{K_0}c_a\left(\frac{\partial\psi}{\partial t}\right)=\frac{\phi\mu_0 c_{a0}}{K_0}\frac{1}{\frac{\mu_0 c_{a0}}{\mu c_a}}\left(\frac{\partial\psi}{\partial t}\right) \tag{29}$$

If $\xi=\frac{\mu_0 c_{a0}}{\mu c_a}$ is recorded, Equation (29) is rewritten as:

$$\frac{\phi\mu}{K_0}c_a\left(\frac{\partial\psi}{\partial t}\right)=\frac{\phi\mu_0 c_{a0}}{K_0}\left(\frac{\partial\psi}{\partial(\xi t)}\right)=\frac{\phi\mu_0 c_{a0}}{K_0}\left(\frac{\partial\psi}{\partial(t^*)}\right) \tag{30}$$

For a single vertical fractured well model, considering the conservation of mass, the following equation is established [11-13]:

$$\xi=\frac{\psi_i-\psi}{\psi_i-\psi^*}=\frac{dt^*}{dt}=\frac{q_{gsc}}{q^*_{gsc}}=\frac{\mu_0 c_{a0}}{\mu c_a} \tag{31}$$

Equation (31) is the core and key of numerical calculation. For steady-state transport, one can use pseudo-pressure to establish familiar formulas for the model, including the flow rate, the pressure distribution, the control region, etc. For non-stationary states, a sufficiently small time unit can be chosen to replace the non-stationary state with a sequence of steady-state flow processes. Of course, more complicated situations can also be considered, such as $\phi=\phi(p)$ and $K=K(p)$, and formula (31) can still be established according to the above method, but the expression of ξ will be more complicated.

3. Parameter Sensitivity Analysis

The related parameters and value range of natural fractured shale gas reservoir are described as follows:

Original shale gas reservoir pressure	$p_{ini}=27MPa$
Original shale gas reservoir temperature	$T_R=331.15k$
Comprehensive permeability of shale gas reservoir	$K_0=0.113\sim20\times10^{-15}m^2$
Average pore throat radius	$r=300\sim4000\times10^{-10}m$
Matrix porosity	$\phi_0=0.05-0.11$
Shale gas reservoir thickness	$h=30m$
Bottom hole flowing pressure	$p_{wf}=6\sim10MPa$
Langmuir volume	$V_L=1\sim10m^3/m^3$
Langmuir pressure	$p_L=0.1\sim10MPa$
Crack half length	$L_f=80m$
Standard condition temperature	$T_{sc}=293.15k$

Comprehensive pressure conductivity coefficient c_a

Standard condition pressure $p_{sc} = 0.101325MPa$

For vertical fracture wells, the relevant literature gives formulas for the calculation and the analysis presented later in this paper is based on this. The values of the relevant parameters are mainly taken from the relevant references, and some authors have considered the parameters to be unreasonable and corrected them. Consider a vertical borehole that has been hydraulically fractured. Hydraulic fracture can be modeled as two fracture surfaces subject to a certain volume flow. The low permeability associated with shale gas formations usually leads to transient behavior from the start of production to abandonment, and the pressure transient rarely extends more than three hundred meters from the well location (Al-Ahmadi et al., 2010). This means that the reservoir can be assumed to be externally unbounded. Thus, the formation can be modeled as two semi-infinite plates, assuming that the flow in the reservoir is linear. The total fracture surface is represented by $4L_f h$, where L_f is a semi-long fracture and h is the formation thickness.

$$\psi(p_{wf}) = \Psi(p_{ini}) - \frac{2q_g T_R p_{sc}}{T_{sc} L_f h} \sqrt{\frac{4t}{\pi \phi c_a \mu K_0}} \tag{32}$$

According to Equation (17), the calculation formulas of deviation factor Z and viscosity μ are introduced. The results show that the compressibility of natural gas does not change much with the decrease of formation pressure during shale gas exploitation, as shown in Figure 1:

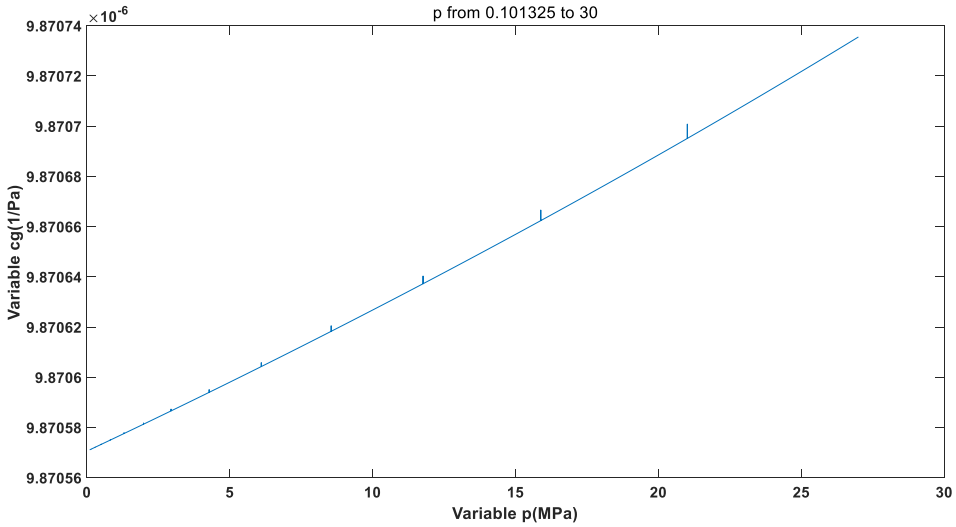

Figure 1 Variation curve of natural gas compressibility with pressure

As can be seen from Figure 1, the compressibility of natural gas remains almost constant and can be regarded as a constant.

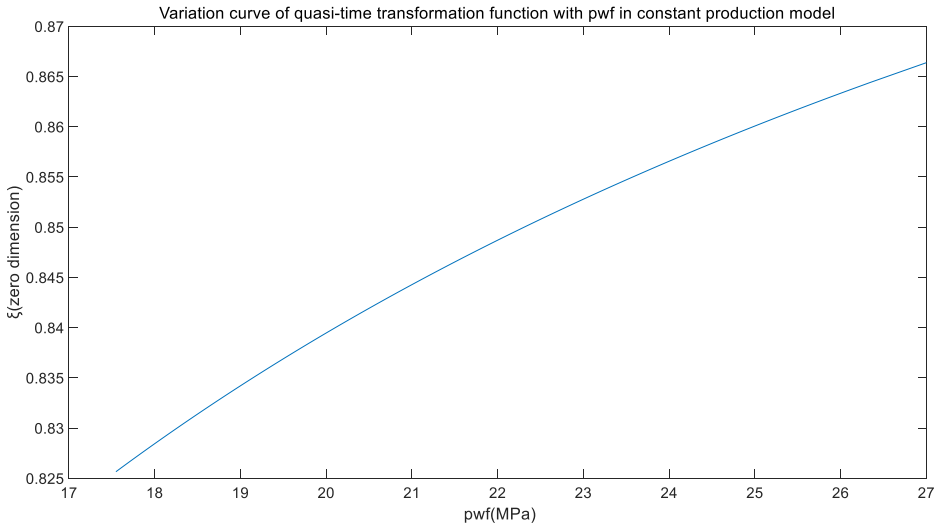

Figure 2 curve of dimensionless pseudo-time transform function with bottom hole pressure

As can be seen in Figure 2, the dimensionless pseudo-time transformation function is clearly affected by the pressure. According to its definition, as the formation pressure decreases, the integrated pressure conductivity decreases and the flow resistance of the shale gas reservoir increases.

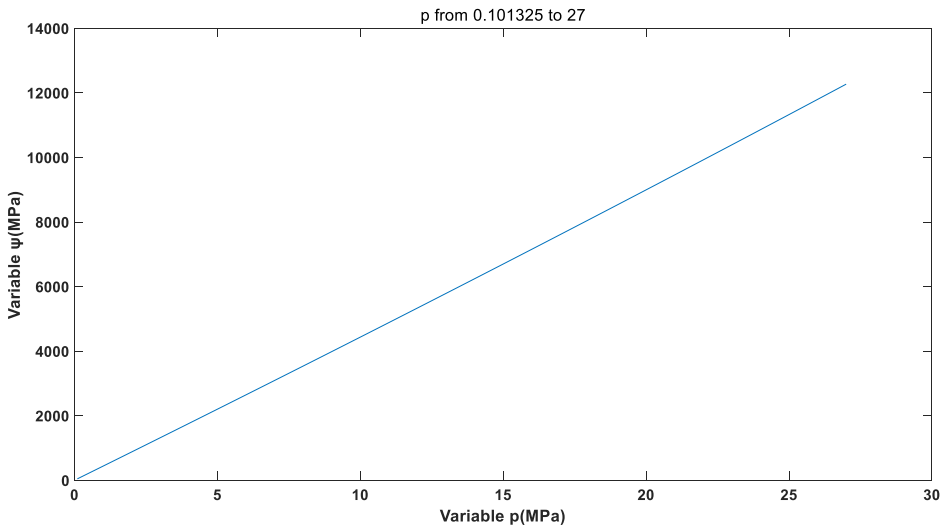

Figure 3 Relationship curve between pseudo pressure and real pressure

The results of the calculation of the pseudo-pressure function are shown in Figure 3 according to the integral definition. From Figure 3, it can be seen that there is a good linear correlation between the real and pseudo pressures, and the relationship between them is almost straight.

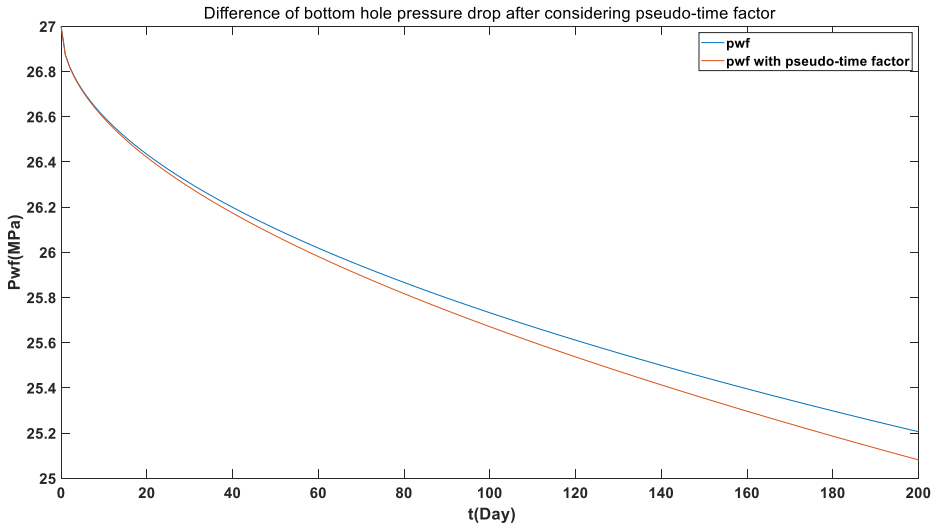

Figure 4 Difference of bottom hole flowing pressure after considering pseudo-time function factor in constant production well test model

Figure 4 shows that there is no significant change in the bottom well flow pressure with and without the pseudo-time factor in the early morning gas well production. From day 20 onwards, the difference between them becomes more pronounced, and the longer the production is practiced, the more significant the difference. In other words, as the production time increases, the integrated pressure conductivity decreases significantly. The reason for this downward trend can be understood as a continuous increase in the resistance of the pressure wave propagation with decreasing pressure, which leads to the need for a larger pressure difference in the nonlinear model to keep the output unchanged.

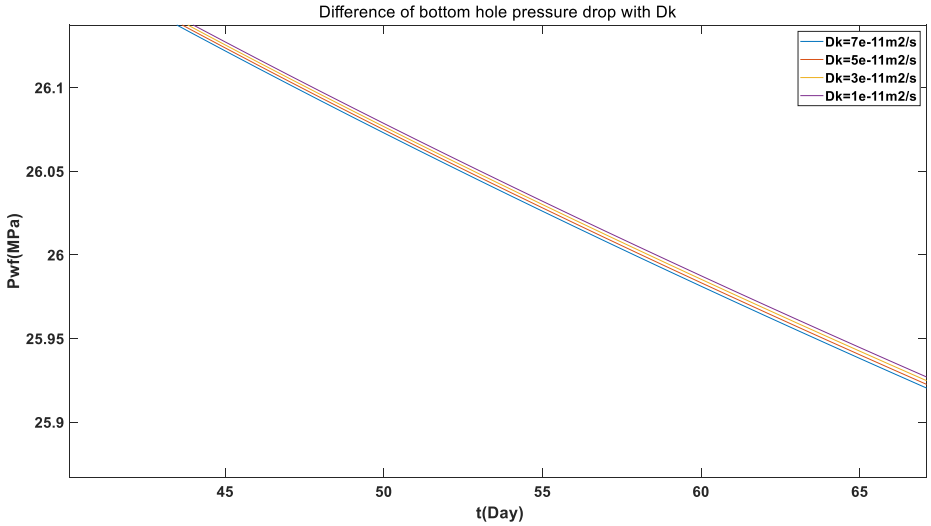

Figure 5 Influence of Knudsen diffusion coefficient on bottom hole flowing pressure

Figure 5 shows that for the constant production well test model, a higher Knudsen diffusion coefficient will always maintain a higher bottom hole flow pressure; at the same time, it also shows that within a reasonable range of experimental values, the difference between them is not significant.

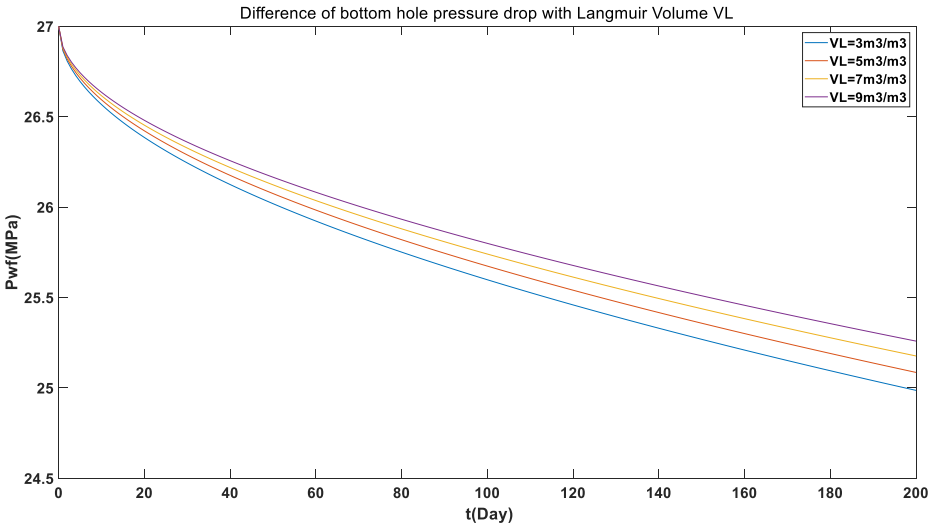

Figure 6 Effect of Langmuir volume on bottom hole flowing pressure

Figure 6 shows that the Langmuir volume has a significant effect on the bottom hole flow pressure. As the Langmuir volume increases, the bottom hole flow pressure decreases, and the difference becomes more and more pronounced as time increases. Therefore, from the point of view of accurate calculations, it is also very important to obtain accurate Langmuir volumes to properly fit the production and development data.

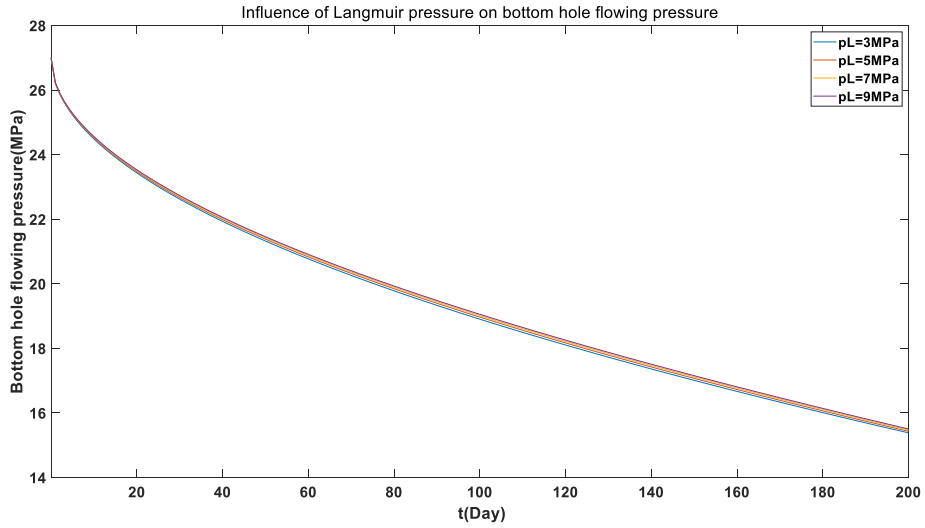

Figure 7 Effect of Langmuir pressure on bottom hole flowing pressure

It can be seen from Figure 7 that a lower Langmuir pressure reduces the bottom hole flow pressure, that is, it is necessary to lower the bottom hole pressure in order to keep the output constant. As can be seen from the figure, this difference increases with time, but it is not significant.

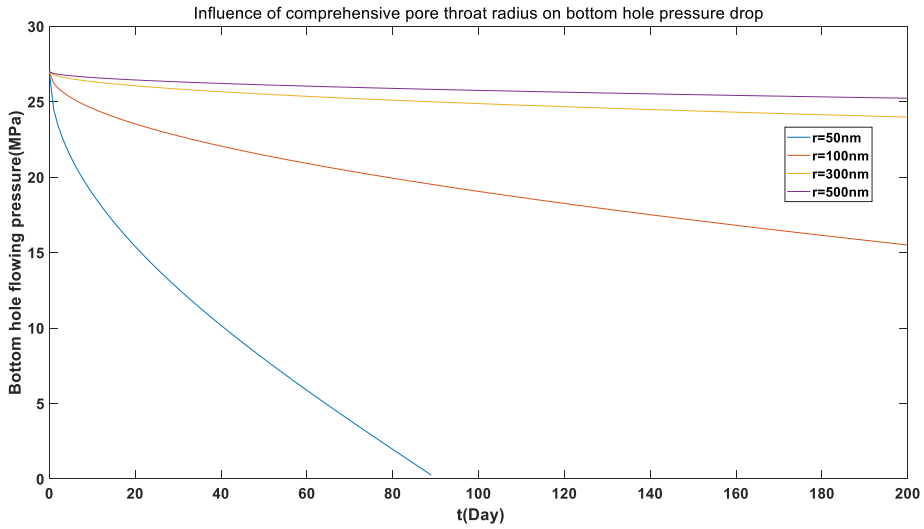

Figure 8 Effect of throat radius on bottom hole pressure drop

This model does not consider fracture systems other than vertical fracture, so the integrated pore throat radius is used to represent natural fractures and microfractures caused by fracture. As can be seen from Figure 8, the effect of the integrated pore throat radius on the bottom hole pressure drop is fatal. The smaller the throat radius, the greater the pressure drop in the bottom hole; however, this difference is significantly reduced when the radius of the pore throat is increased to some extent, which provides a reasonable basis for the reconstruction of this reservoir.

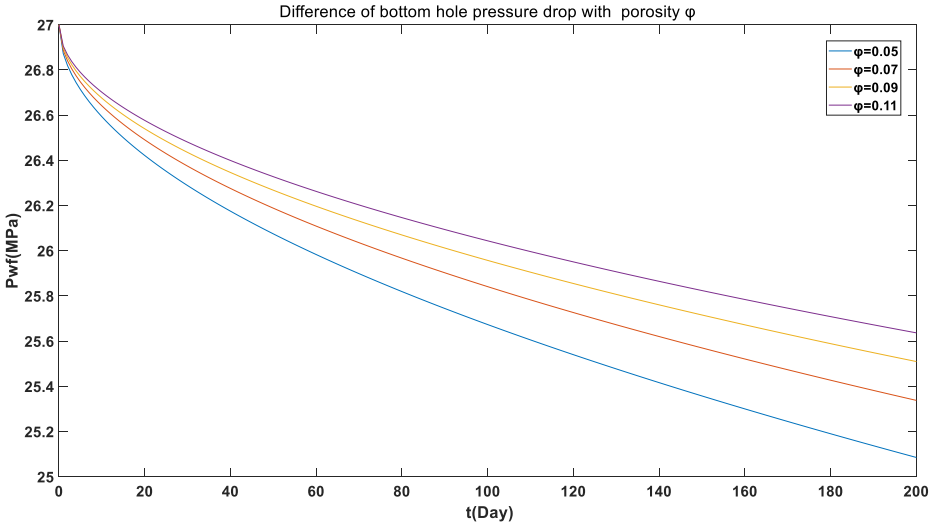

Figure 9 Influence of porosity on bottom hole pressure drop

Figure 9 shows that the bottom hole pressure drop decreases with increasing porosity; The lower the porosity, the larger the amplitude of the pressure drop with time. The porosity distribution, the integrated pore throat radius, and the permeability are all correlated, so probability theory has been given to characterize these parameters in the relevant literature. If large-scale volumetric fracturing is used, the pore volume will increase, which will have an impact on production. In conjunction with Figure 8, we argue that it is more important to keep the formation pressure at a high level, avoid fracture closure, and keep the integrated pore radius of the formation at a high level, which is more conducive to production.

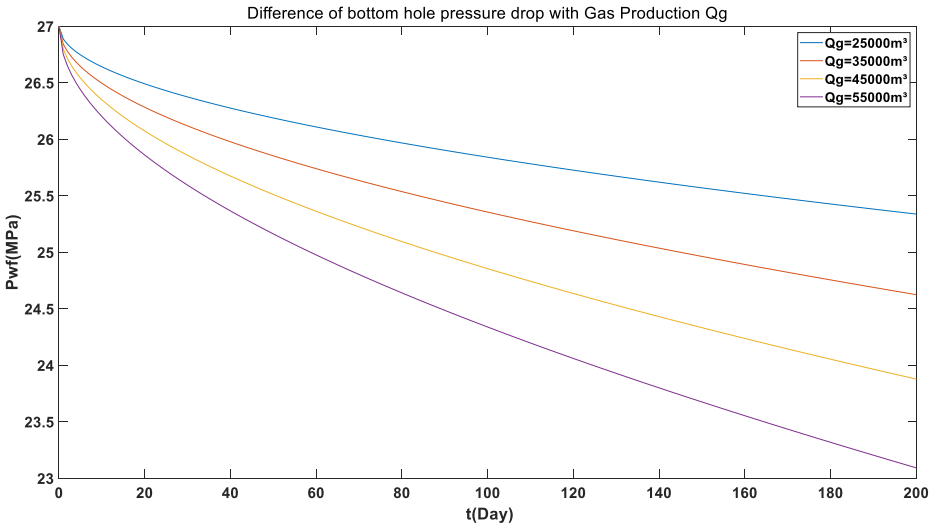

Figure 10 Variation law of bottom hole pressure with time under different trial production output

As can be seen in Figure 10, the bottom hole pressure tends to stabilize with increasing time; the smaller the trial production, the shorter the time to enter steady-state percolation, and vice versa.

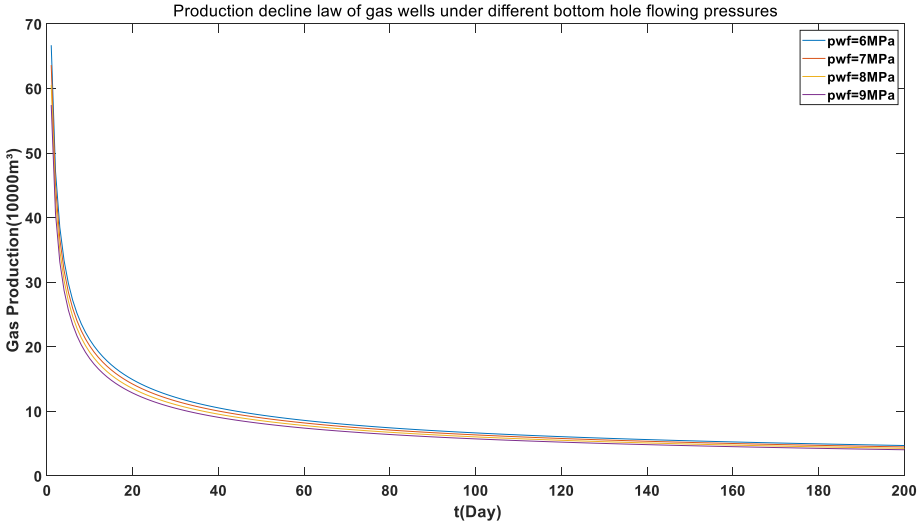

Figure 11 Production decline law of gas wells under different bottom hole pressures

Figure 11 shows that the difference in production at different bottom hole pressures has different characteristics at different stages. At the initial stage of production, the difference is relatively large, and it gradually becomes smaller as the time increases. This law of variation can be explained by the control radius theory:

$$q_g = \frac{2\pi K_0 h}{\mu} \frac{\Psi_i - \Psi_w}{\ln \frac{r_{et}}{r_{wf}}} \tag{32}$$

Where ψ_i and ψ_w are the pseudo pressure at the boundary and the pseudo pressure on the bottom hole fracture surface respectively, r_{et} is the control radius of vertical fracture well, which increases with time, and r_{wf} is the converted radius of vertical fracture, which can be converted into circular radius according to the equal length.

According to Equation (32), the pseudo-pressure difference is fixed, and the influence of pseudo-pressure difference is great in the early stage because of the small control radius; when the control radius increases

gradually, the denominator in equation (32) increases continuously, so the difference of selecting different pseudo-pressure differences for production will no longer be obvious. At the same time, we can see that after a certain period of production, output tends to stabilize.

As can be seen from Figure 12, the Langmuir pressure has a significant effect on the early time, and the smaller the Langmuir pressure, the larger the early time. Figure 13 shows that the yield relation between the different Langmuir pressures does not change significantly after a long period of production. This result suggests that Langmuir desorption and percolation are parallel, with a larger contribution from desorption at low Langmuir pressure. From the computational model, it can be seen that the Langmuir pressure affects the output by affecting the integrated pressure conductivity, that is, a low Langmuir pressure will increase the pressure conductivity and reduce the flow resistance, leading to a higher output; for sufficiently long times, its effect on the pressure conductivity becomes smaller as the control radius increases.

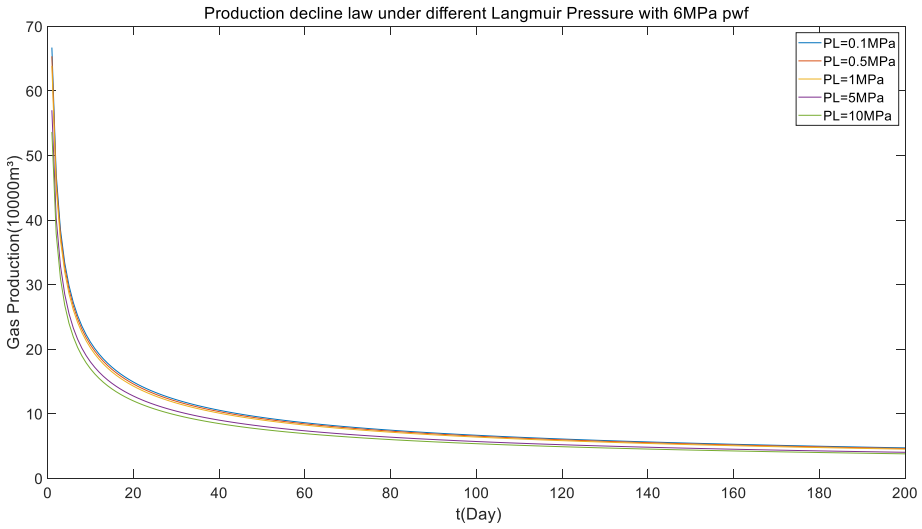

Figure 12 Production decline law under different Langmuir pressures (full picture)

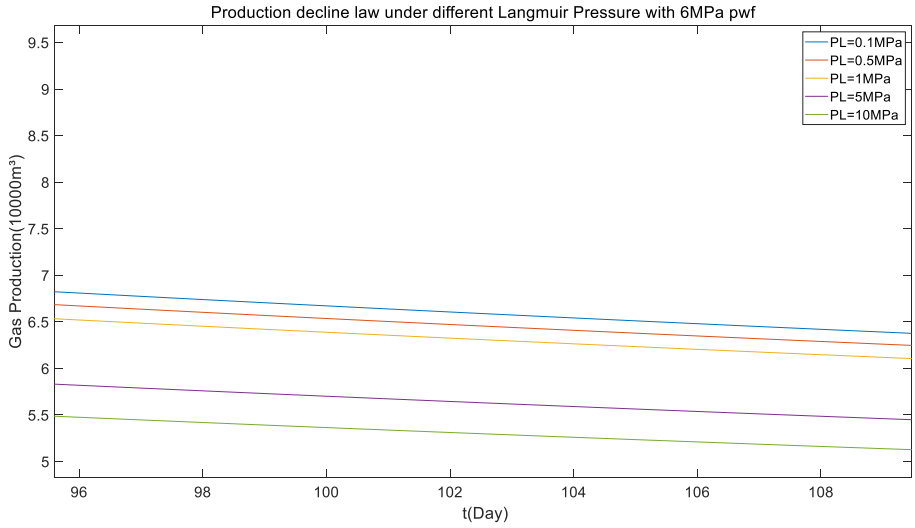

Figure 13 Production decline law under different Langmuir pressures (partial enlarged view)

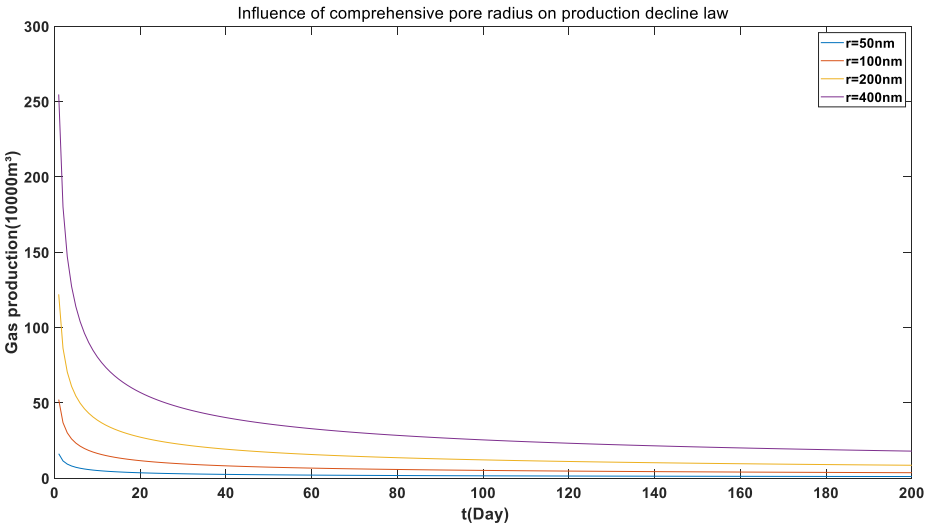

Figure 14 Influence of comprehensive pore throat radius on production decline law

Based on Figure 14, it can be found that the effect of the integrated pore radius on productivity is very significant in both the early and steady stages of production. The smaller the throat radius, the lower the productivity. For shale gas reservoirs, it is important for production to transform the reservoir and keep the formation pressure high enough to keep the microfracture open.

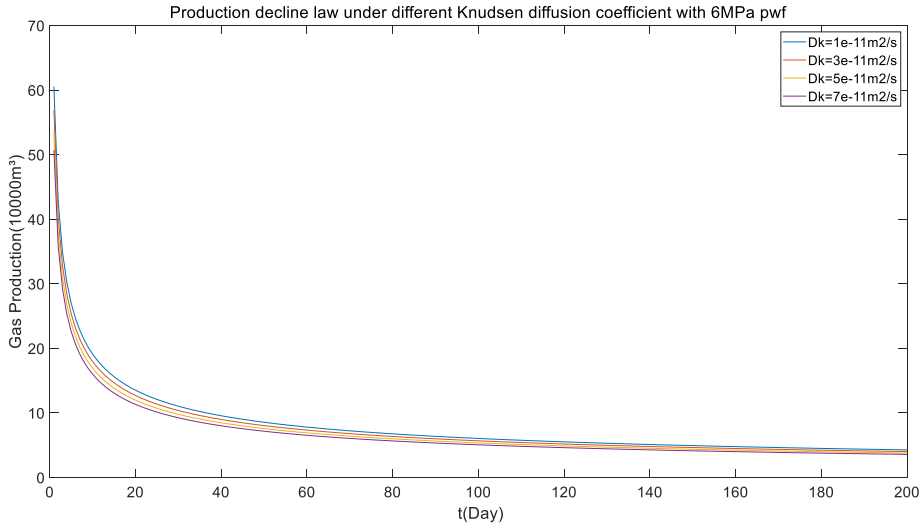

Figure 15 Influence of knudsen diffusion coefficient on production decline law

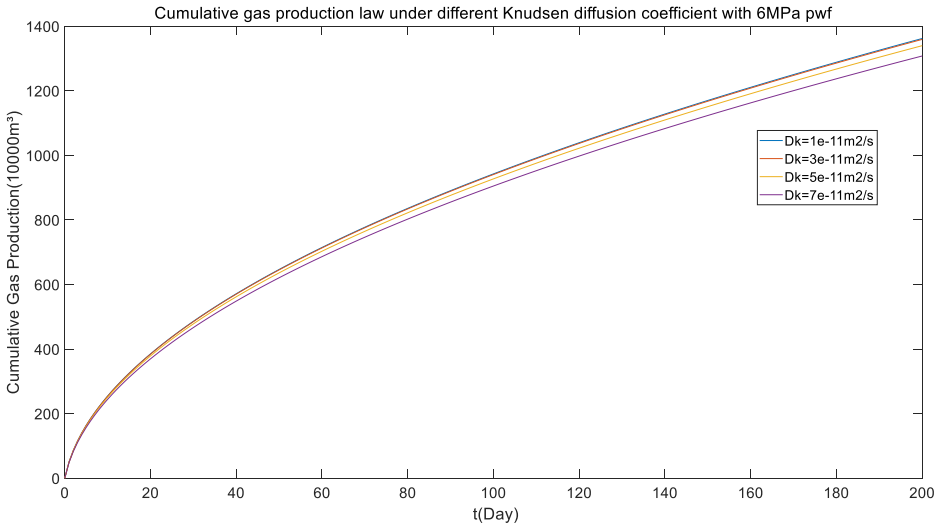

Figure 16 Influence of knudsen diffusion coefficient on cumulative gas production

As can be seen from Figures 15 and 16, the smaller the Knudsen diffusion coefficient, the higher the productivity, and vice versa.

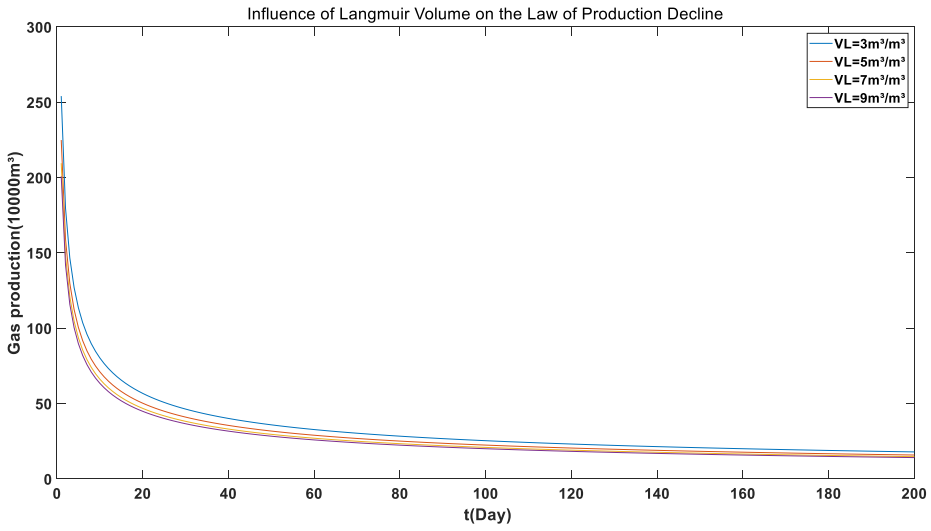

Figure 17 Effect of Langmuir volume on production decline law under the condition of constant bottom hole flowing pressure

It can be seen from Figure 17 that a lower Langmuir volume is beneficial for reducing the transport resistance of shale gas in the formation, but it is clear that this resistance decreases as the control area increases.

4. Conclusion

The results of the numerical calculations and analysis show that the linearized approach presented in this paper is consistent with the inherent logic of mathematical and physical models of shale gas reservoirs and therefore can be trusted. The analysis shows that the biggest influence lies in the pore structure of the shale gas reservoir itself, whether successful reservoir reconstruction measures have been taken and whether a reasonable working system has been adopted.

1. The introduction of pseudo-pressure transformation function can accurately calculate the variation of comprehensive conductivity with pressure and time, and the traditional seepage equation can still be used as the

basis for considering the multi-scale transport equation of desorption shale gas reservoir, such as production decline, bottom hole pressure change and formation pressure redistribution.

2. The quasi-time transformation function is mainly based on the comparison of the pressure conductivities. It replaces the non-stationary processes with a series of stationary processes, one by one. In the calculation, it is necessary to assume that the pressure conductivity is invariant and then modify the boundary conditions. These corrections are essentially corrections to the pressure conductivity coefficients, which are then built into the mass conservation equations to obtain the true pressure and yield by using the assumption of transient stability.

3. It is easy to obtain the conversion relation between the pseudo and real pressures by the definition of integral equations. The results show that for shale gas there is a good linear correlation between the real and pseudo pressure.

4. Although porosity, permeability, and integrated pore throat radius can have a large effect on production, these parameters are not independent. Establishing statistical relations between these parameters is very important and fundamental work;

5. According to the calculation of Langmuir pressure in the experimental measurement range, the production pressure drop and the production decline change of the fixed well test model are not significant, which mainly affect the early production, which is related to the small control radius of the early production area, but the impact is limited;

6. According to the calculation within the range of Langmuir volume provided by the literature, the results show that: 1) under the condition of constant production, the smaller Langmuir volume, the lower the bottom hole flowing pressure, and the results calculated by different numbers will increase with the increase of time; 2) under the condition of constant bottom hole flowing pressure, the smaller Langmuir volume, the higher the output, and the difference of the results calculated by different numbers will decrease with the increase of time.

References

[1] X. He, W. G. Li, L.R. Dang, et al., “Key technological challenges and research directions of deep shale gas development,” Natural Gas Industry, vol. 41, no. 1, pp. 118-124, 2021.

[2] J Yang, Y L Kang, Y Sang, et al., “Research on diffusibility of the gas in tight sand gas reservoir,” Southwest Petroleum University: Science &Technology Edition, vol. 31, no. 6, pp. 76, 2009.

[3] Z. S. Wang, “Study on mechanism and discontinuous deformation analysis of hydraulic fracturing of rock,” Jinan:Shandong University, 2019.

[4] G.G. Michel, R. F. Sigal, F. Civan and D. Devegowda, “Parametric investigation of shale gas production considering nano-scale pore size distribution, formation factor, and non-darcy flow mechanisms”, SPE147438, SPE Annual Technical Conference and Exhibition, 2011a, pp. 1-20.

[5] F. A. Civan, “Triple-mechanism fractal model with hydraulic dispersion for gas permeation in tight reservoirs”, SPE 74368, SPE International Petroleum Conference and Exhibition, Villahermosa, Mexico, 2002, pp. 10-12.

[6] F. Civan, “Effective Correlation of Apparent Gas Permeability in Tight Porous Media,” Transport in Porous Media, vol. 82, no. 2, pp. 375-384, 2010a.

[7] F. Civan, “A review of approaches for describing gas transfer through extremely tight porous media”, Third International Conference on Porous Media and its Applications in Science, Engineering and Industry, 2010b, pp. 395-399.

[8] E. A. Guggenheim, Elements of the Kinetic Theory of Gases, Pergamon Press, USA: New York, 1960.

[9] C. M. Freeman, G. J. Moridis, T. A. Blasingame, “A numerical study of microscale flow behavior in tight gas and shale gas reservoir systems,” Transp Porous Med, vol. 90, pp. 253–268, 2011.

[10] J. Deng, “Nonlinear seepage theory of multistage fractured horizontal wells for shale gas reservoirs,” PhD dissertation, Fluid mechanics, Beijing University of Science and Technology, 2015.

[11] Z. C. Liao, “Analytic methods and application on nonlinear porous flow groups,” PhD dissertation, Fluid mechanics, University of Chinese Academy of Sciences (Institute of Seepage Fluid Mechanics, Chinese Academy of Sciences) , 2015.

[12] Z. C. Liao, “A new solution of the non-linear flow equation for ultra-low permeability reservoirs,” Int. J. Simul. Syst. Sci. Technol, vol. 17, no. 45, pp. 2.1-2.6, 2016.

[13] Z. C. Liao. “A new solution to the seepage equations in deformed media,” Proceedings of the 9th Academic Conference of Geology Resource Management and Sustainable Development, 2022.